Three-dimensional modelling of anchorage zones in reinforced concrete

(article starts on next page)

THREE-DIMENSIONAL MODELLING OF ANCHORAGE ZONES IN REINFORCED CONCRETE

K. Lundgren[1] and J. Magnusson[2]

1) Assistant Professor, Division of Concrete Structures, Chalmers University of Technology, SE-412 96 Göteborg, Sweden. 2) Ph.D., Division of Concrete Structures, Chalmers University of Technology, and AB Jacobson & Widmark.

ABSTRACT: A model describing bond between deformed reinforcement bars and concrete was developed, which considers the splitting stresses of the bond action. The model was previously verified against pull-out tests of various geometries. In this study it is used in three-dimensional finite element analyses of different anchorage situations. One application was lapped reinforcement splices, in beams and in frame corners. Another application was bars anchored in beam-ends with varying support conditions. When no additional confinement from the support reaction was present, splitting cracks appeared, which reduced the anchorage capacity both in the analyses and in the tests. Analyses and tests of the anchorage at end regions of simply supported beams showed that the main part of the tensile force transfer between reinforcement and concrete takes place above or close to the support. It can be concluded that the bond model could describe the behaviour of the different anchorage situations for both normal- and high-strength concrete in a satisfactory way, and thus can be used for further studies of different anchorage situations.

Key words: Reinforced concrete, Anchorage, Bond model, Finite element analyses, Splitting effects, Support conditions, Lapped splice, Non-linear fracture mechanics.

BACKGROUND

When reinforced concrete structures are analysed, perfect bond between the reinforcement and the concrete is perhaps the most frequent assumption. Especially when the overall behaviour of a larger structure is examined, this assumption is often sufficient. Nevertheless, if one is interested in following the crack development more thoroughly, the bond mechanism needs to be taken into account. The most usual way to do this is to employ bond versus slip relations as input. However, the bond versus slip depends on the structure and its response. To assume a reasonable bond versus slip relation is difficult; parameters such as the actual concrete cover, the amount of transverse reinforcement, and whether the reinforcement will begin to yield, need to be taken into account. Yet, if one wishes to study crack development in structural members, for example, then this way of taking the bond mechanism into account offers a sufficient level of accuracy and detail.

However, for more detailed analyses of parts of a structural member where the bond mechanism plays a decisive role, a more refined model for the bond is needed. This is needed mainly for analyses of anchorage regions, such as in splices and anchorage of the reinforcement at end regions, but also for analyses of the rotational capacity, where the bond plays a crucial part. A requirement for this type of model is that the bond mechanism is described in such a way that the bond versus slip achieved in a structure is a result of the analysis, rather than an input. Another requirement is that the model includes not only the bond stresses, but also the splitting stresses that result from the anchorage. Two such models that can be used in finite element analyses have been found in the literature: the model by Åkesson (1993) and the one by Cox and Herrmann (1998, 1999), see also Cox (1994). They are both elasto-plastic models, with yield surfaces to limit the stresses. A drawback to Åkesson's model is that there is no upper limit of the bond stress; the bond stress can thus become infinitely high as long as enough normal stress is present. This does not agree with the experimental results of, for example, Robins and Standish (1984). Their tests showed that lateral confinement changed the failure mode from splitting failure to pull-out failure. Yet, further increase of the lateral confinement had no effect on the bond capacity. The model by Cox (1994) does not have this drawback. This model is a more general model of the bond mechanism than the model by Åkesson.

In the present work, a new model which directly uses the basic mechanisms to describe the yield surface was used. As the models of Åkesson, and Cox and Herrmann, it is suited for detailed three-dimensional analyses. The splitting stresses caused by the bond action are included, and the bond stress depends not only on the slip, but also on the radial deformation between the reinforcement bar and the concrete. Thereby, the influence of the surrounding structure is included, so that the bond stress will decrease if the concrete splits, or the reinforcement starts yielding. The model used was earlier verified against pull-out tests with various geometry and with both monotonic and cyclic loading; see Lundgren and Gylltoft (2000). Here, results from finite element analyses of anchorage regions in larger structures are presented and compared with test results.

THEORETICAL MODEL

The theoretical model is briefly presented here; for more details see Lundgren and Gylltoft (2000), or Lundgren (1999). In the finite element program DIANA, there are interface-elements available, which describe a relation between the traction **t** and the relative displacement **u** in the interface. These interface elements are used at the surface between the reinforcement bars and the concrete. The physical interpretations of the variables t_n, t_t, u_n and u_t are shown in Fig. 1.

The model is a frictional model, using elasto-plastic theory to describe the relations between the stresses and the deformations. The yield surface is defined by two functions, one describing the friction F_1, assuming that the adhesion is negligible. The other yield function, F_2, describes the upper limit at a pull-out failure. F_2 is determined from the stress in the inclined compressive struts that results from the bond action, see Fig. 2.

$$F_1 = |t_t| + \mu t_n = 0 \qquad (1)$$

$$F_2 = t_t^2 + t_n^2 + c \cdot t_n = 0 \qquad (2)$$

The yield surface is shown in Fig. 2. For plastic loading along the yield function describing the upper limit, F_2, an associated flow rule is assumed. For the yield function describing the friction, F_1, a non-associated flow rule is assumed, for which the plastic part of the deformations is

$$d\mathbf{u}^{\mathrm{p}} = d\lambda \frac{\partial G}{\partial \mathbf{t}}, \qquad G = \frac{|u_t|}{u_t} t_t + \eta t_n = 0 \qquad (3)$$

For the hardening rule of the model, a hardening parameter κ is established, approximately equal to the applied slip. The variables μ and c in the yield functions are assumed to be functions of κ. The coefficient of friction, μ, is assumed to vary from 1.0 down to 0.4 during the hardening, and the stress in the inclined compressive struts, c, is chosen to be the same as the uniaxial compression curve of the concrete. The parameter η is assumed to be constant for monotonic loading. The model can also be used for cyclic loading.

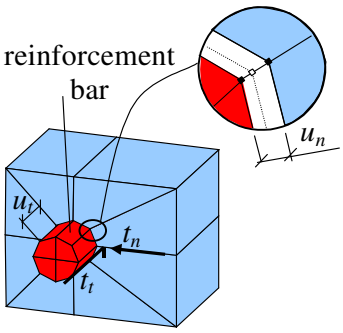

$$\mathbf{t} = \begin{bmatrix} t_n \\ t_t \end{bmatrix} = \begin{bmatrix} \text{normal splitting stress} \\ \text{bond stress} \end{bmatrix}$$

$$\mathbf{u} = \begin{bmatrix} u_n \\ u_t \end{bmatrix} = \begin{bmatrix} \text{relative normal displacement at the layer} \\ \text{slip} \end{bmatrix}$$

Figure 1 Physical Interpretation of the Variables t_n, t_t, u_n and u_t.

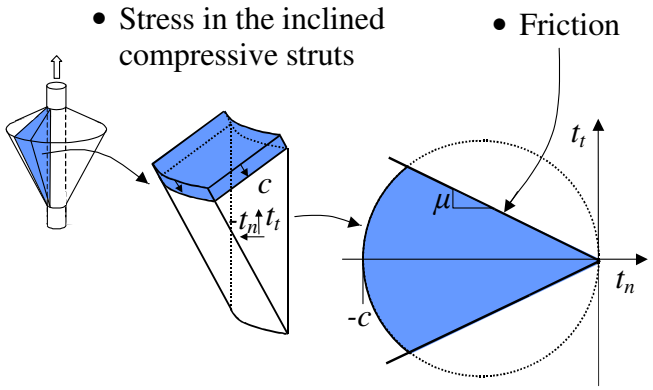

Figure 2 The Yield Surface of the Theoretical Model.

FINITE ELEMENT ANALYSES OF ANCHORAGE REGIONS

Three-dimensional finite element analyses of anchorage regions were carried out. The concrete and the main reinforcement were modelled with eight-node solid elements, using non-linear fracture mechanics and a rotating crack model based on total strain for the concrete; see TNO (1998). The deformation of one crack was smeared over a length corresponding to the size of one element. The hardening in compression was described by the expression of Thorenfeldt *et al.* (1987). Necessary material data for the concrete were estimated, according to the expressions in CEB (1993) and CEB (1995), from the compressive cylinder strength. For the tension softening, the curve by Hordijk *et al*. was chosen, as described in TNO (1998). The constitutive behaviour of the reinforcement steel was modelled by the von Mises yield criterion with associated flow and isotropic hardening. The yield capacity of the steel was approximately 500 MPa. For more information about the properties of the reinforcement, see Magnusson (2000) and Lundgren (1999). The compressive and the transverse reinforcement were modelled as “embedded” reinforcement, meaning that perfect bond between the concrete and the reinforcement was assumed. The bond mechanism between the concrete and the main reinforcement bars was described by the new model using special interface elements.

Table 1 Results from Tests and Analyses of Beams with Lapped Tensile Splices

Beam number	Stirrups	$f_{c\,cyl}$ [MPa]	Failure load Q_{max} [kN]	Mid-span Displ. at Q_{max} [mm]	Tensile force [1)]		
					Outer corner bars [kN]	Centre bar [kN]	Inner corner bars [kN]
NSC-45	-	27.0	90.7	5.0	56.8 / 56.1	56.1 / 64. 9	50.7 / 79.3
analysis			83.0	6.3	44.3	71.5	49.0
NSC-47	5ø6 s90	29.3	107.2	6.8	70.0/ 71.2	74.7 / 83.0	81.8 / 82.2
analysis			135.2	11.7	86.1	107.2	95.5
NSC-49	9ø8 s45	30.3	142.4	11.1	119.9 / 117.7	76.4 / 65.6	120.4 / 120.9
analysis			161.5	13.2	104.9	116.0	127.2
HSC-45	-	61.3	79.8	3.9	37.8 / 38.6	53.7 / 70.2	54.6 / 67.7
analysis			87.0	5.0	45.9	56.0	52.7
HSC-47	3ø8 s80	62.0	99.8	5.4	60.2 / 46.9	51.1 / 76.9	64.1 / 49.0
analysis			117.3	8.9	66.4	78.3	82.0
HSC-49	6ø10 s32	62.7	167.4	10.8	127.0 / 123.3	—/ 112.7	97.7 / 124.6
analysis			152.6	11.2	85.2	103.9	115.9

[1)] Two values from the test, since the force was measured on each end of the splice. One value from the analyses, due to the assumed symmetry.

Lapped reinforcement splices

Splices in beams

Tests and analyses of the anchorage in splice regions were carried out. A total of sixteen beams were tested; six of these were analysed and will be discussed in greater detail here. For more information about the tests, see Magnusson (2000). The beams had tensile reinforcement spliced in the mid-span, and the effect of transverse reinforcement along a fully lapped splice was studied. The beams were simply supported and loaded in four-point bending, with a shear span of 420 mm and a free span of 2.0 m. They were 200 mm wide and 240 mm deep. The splice lengths used were 200 mm for the high-strength concrete beams and 400 mm for the normal-strength concrete beams; this was done to obtain splice failure, and so that the splice strength would be approximately the same for both concrete types.

All of the beams were under-reinforced with three K500ST ø20 bars provided as tensile reinforcement, and with a compressive reinforcement of two K500ST ø16 bars. The clear concrete cover to the tensile reinforcement was 20 mm. Stirrups of the reinforcement type K500 ST (ø6, ø8 and ø10) were used, with spacing along the splice as shown in Table 1. To ensure that the failure occurred in the mid-span, welded transverse cross-bars were used at the support.

The finite element mesh used in the analyses is shown in Fig. 3. To reduce the time required to run the analyses, only half of one beam was modelled, using the symmetry line in the mid-span. The deformations of the reinforcement bars at the mid-

span were tied to each other as can be seen in the enlarged part in Fig. 3. In the tests, the corner reinforcement bars from one half of the beam were both outer reinforcement bars. However, in the modelled beam half, the corner reinforcement bars were one outer and one inner corner bar, in order to be able to use a symmetry line at mid span. Since the splice length differed between the beams with normal-strength concrete and high-strength concrete, the mesh was adjusted for that. The only other feature that differed between the tests was the amount of stirrups along the splice; since the transverse reinforcement was modelled as embedded reinforcement, this could be adjusted without changing the mesh.

In all of the tests on beams with spliced reinforcement, as well as in the analyses, fracture of the splice limited the capacity. An example of a crack pattern obtained in an analysis is shown in Fig. 3. Bending cracks along the beam appeared at first; thereafter splitting cracks at the splice reached the outer surface. When there was no transverse reinforcement along the splice, this occurred at maximum load. However, when there was transverse reinforcement, the load could be increased after the splitting cracks had penetrated the cover. In all of the analyses, the splitting cracks resulted in longitudinal cracks following the reinforcement bars on the bottom face of the beam. At the maximum load, the bending crack at the end of the splice became very large in all of the analyses. This behaviour corresponds well with what was observed in the tests.

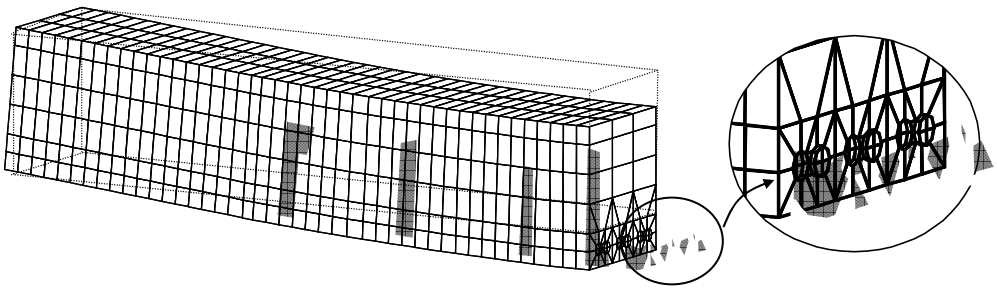

Figure 3 The Finite Element Mesh used in the Analyses of the Beams with Lapped Splices. Results are from the Analysis of HSC-45, at the Maximum Load. Grey Marked Regions Indicate Cracked Concrete.

A comparison of the load versus mid-span deformation from the tests and the analyses is shown in Fig. 4. As can be seen, the agreement is rather good, even though the capacities of the NSC-47 and HSC-47 are slightly overestimated. An example of the stress distribution along a splice is shown in Fig. 5, from the analysis of NSC-49, at the maximum load. There, it can be seen how the stress increased in the reinforcement bar along the splice length. The maximum stress in the reinforcement bar, at the lower edge of it, and the minimum stress, at the upper edge, are also indicated. It can be seen that the difference is increasing towards the end of the splice. This is due to the large bending crack at the end of the reinforcement splice, and because the reinforcement carried a small part of the moment. This local bending of the reinforcement was noted in all of the analyses on splices, and is probably one reason why the tensile forces in the reinforcement bars evaluated from the tests varied rather widely, see Table 1. These tensile forces were evaluated from measurements of strain gauges, one on each reinforcement bar at the end of the splice.

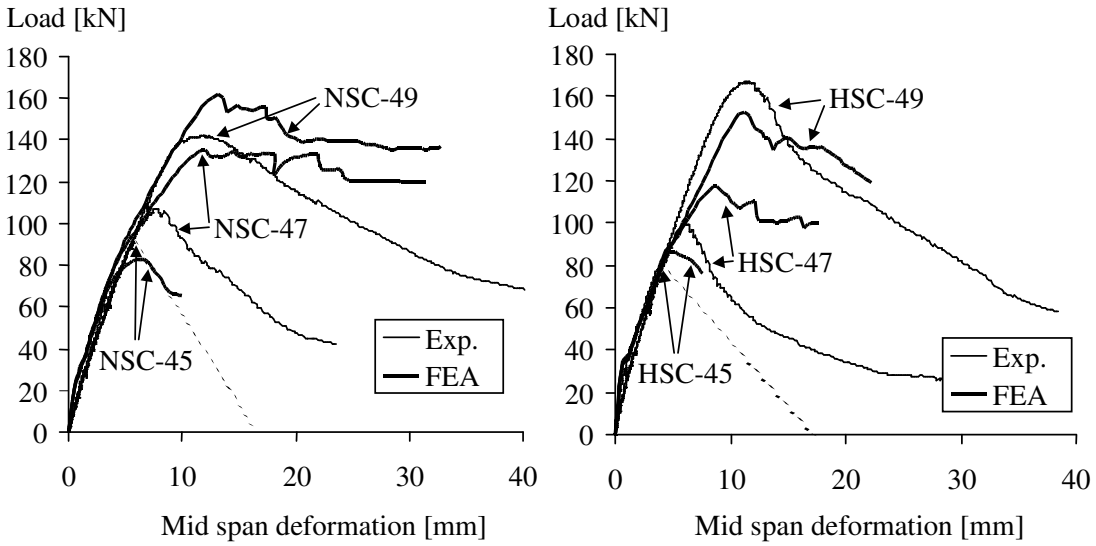

Figure 4 Comparison of Test Results and Analyses of the Anchorage in Splice Regions. The Descending Part of the Load in the Tests NSC-45 and HSC-45 are Dotted, since it Could not be Followed in the Tests.

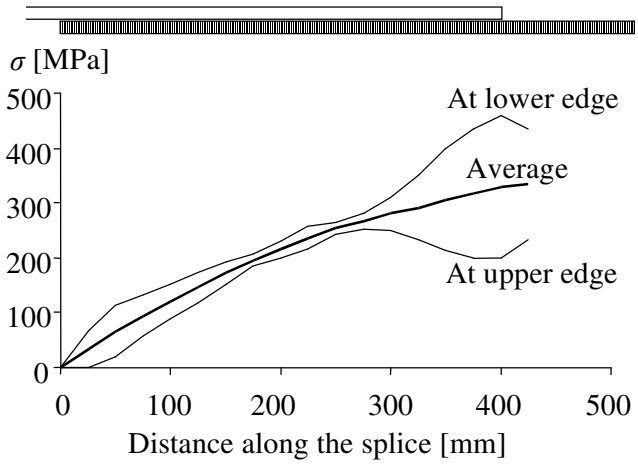

Figure 5 Stress Distribution along a Splice. Results from the Analysis of NSC-49, from the Outer Corner Bar.

In Fig. 6 (a), the bond stress distribution from the analyses, at the maximum load, is shown. The bond stress was calculated from the average of the steel stress distribution in all of the three bars in a cross-section. This means of presenting the bond stress was chosen since the difference between the bars was rather small. The influence of increased transverse reinforcement and increased concrete strength upon the bond stress are clearly shown. The decrease of the bond stress towards the end of the splice depends on the bending crack that appears there. At the bending crack, the slip changes direction and therefore decreases to zero, as can be seen in Fig. 6 (b); and with small slip, the bond stresses also become very small. In reality, the change in slip direction would be very sudden near the crack; however, in the analyses, the change in slip direction takes place in one or two elements, which leads to a more gradual decrease in slip. In Fig. 6 (b), it can also be noted that the slip at the maximum load in the beams without stirrups along the splice was markedly smaller than in the beams with stirrups. This is especially true for the high-strength concrete. This is because stirrups provide a possibility of stress redistribution, thus resulting in an increased ductility.

In conclusion, the overall behaviour of the analysed beams corresponded well with the response of the tested beams. The increase in strength and ductility of the splices due to the confinement of the stirrups was described in a reasonable way. Furthermore, the analyses could give information about the bond stress and the slip distribution along the splices.

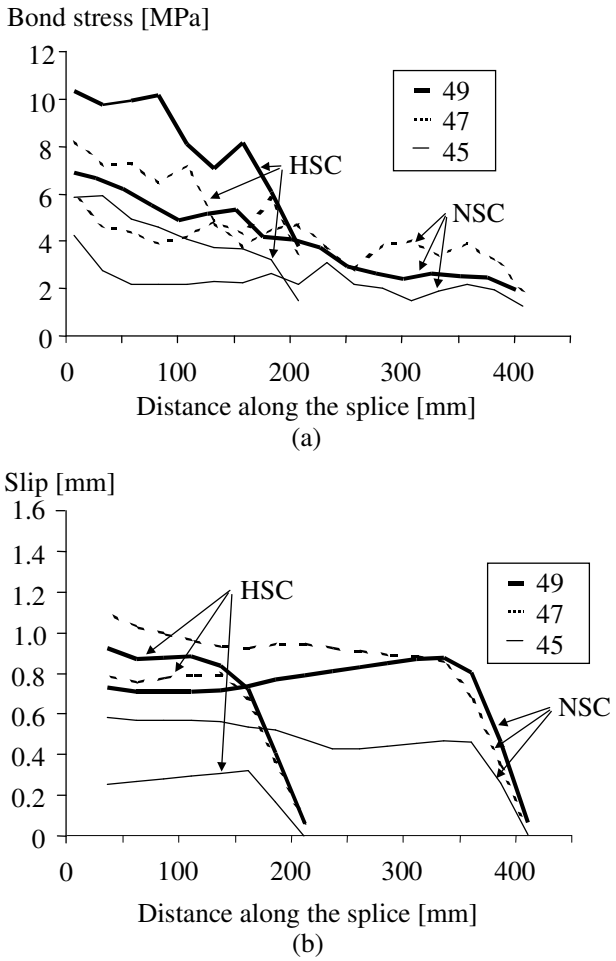

Figure 6 (a) Average of the Local Bond Stress Distribution, and (b) Average Slip Distribution, along the Splices from the Analyses, at the Maximum Load.

Splice in corner region

The bends of the reinforcement bars in corners generate splitting stresses perpendicular to the plane of the bend. When the reinforcement is spliced, additional splitting stresses arising from the anchorage of the reinforcement could decrease the bond capacity. By using detailed three-dimensional models, combined with the new model for the bond, these effects could be taken into account in the analyses. Four frame corners were tested and analysed for a closing moment; here, however, only one of them, where the splice capacity was limiting, will be discussed. For more information, see Lundgren (1999). The geometry of the detailing in the corner region is shown in Fig. 7 (a), and the tested and analysed load case is shown in Fig. 7 (b). The concrete had a compressive strength of 34 MPa. To limit the size of the model, only a thin slice of the frame corner was modelled. It had one reinforcement bar (in

the splice, two), and was extending halfway to the next reinforcement bar. Two analyses were carried out, for a centre slice and for an edge slice, with boundary conditions as shown in Fig. 7 (c). In the specimen tested, there were ten reinforcement bars. To enable comparisons between the analyses and the tests, the load obtained from the analyses of thin slices was multiplied by ten.

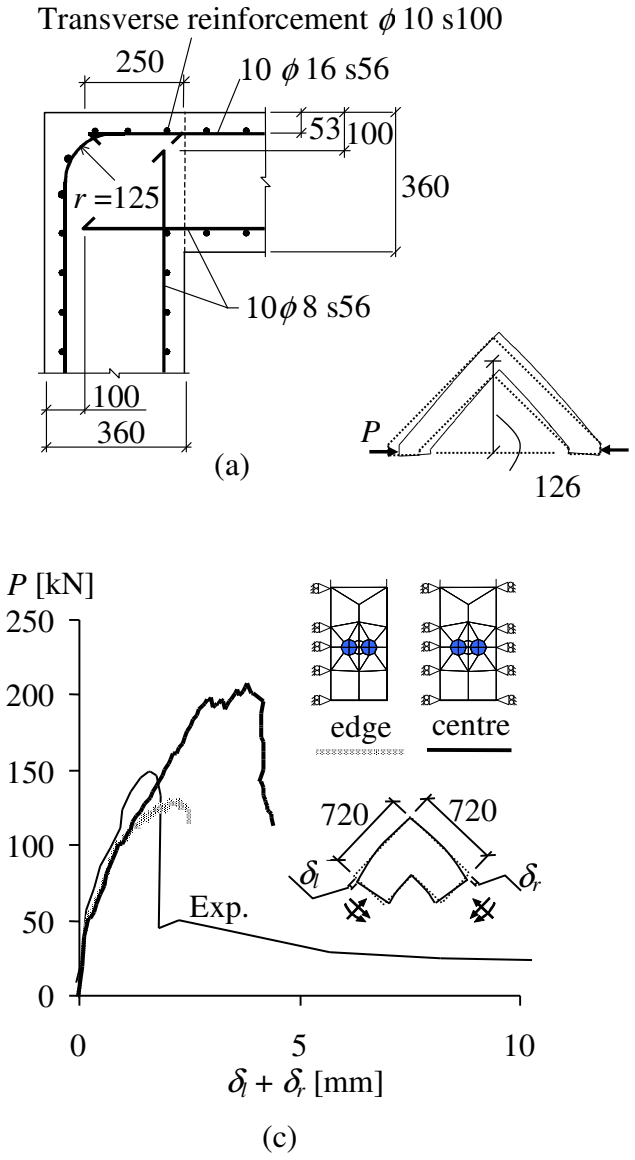

Figure 7 (a) Detailing in the Corner Region; Measurements in mm, (b) Tested and Analysed Load Case, and (c) Comparison of Test Results and Analyses.

In the experiment, the cracks around the splice were noted when the load was about 135 kN, and maximum load was obtained at 150 kN. In the analysis of a centre slice, cracks splitting the cross-section into two parts at the level of the reinforcement developed from the spliced reinforcement bars, and reached the symmetry lines at a load about 120 kN. The load could, however, continue to increase, since bond could still be carried along the sides of the reinforcement bars. When a load of about 200 kN was obtained, the capacity of the splice was reached; see Fig. 7 (c). In the analysis of an edge slice, the splitting crack was formed at a load corresponding to about 110 kN for the whole specimen, i.e. a load only slightly lower than that of the centre slice. The main difference between the two analyses was that, when there was a free edge, the load could not be increased much after the splitting crack had formed; the maximum load obtained was only 128 kN. As can be expected, the test results lie between the two analyses, see Fig. 7 (c), but closer to the analysis results from the edge slice. This indicates that when the outer reinforcement splices reach their capacity, the next reinforcement splices loose some of the support action from them. In this way, fracture of the splice is spread from the edges towards the centre.

Anchorage in end regions

The anchorage of ribbed bars in end regions has been investigated in an extensive study, consisting of both experiments and FE-analyses. The specimens tested and analysed were idealised beam-ends and simply supported beams subjected to four-point bending. In the beam-ends it was possible to study the influence of different support conditions under rather pure conditions. In the beam tests, on the other hand, the anchorage could be studied under more realistic load conditions, and the possibilities for stress redistribution could be studied. The study was carried out using two concrete types, a normal-strength and a high-strength concrete with cylinder compressive strengths of about 25 MPa and 100 MPa respectively. For more detailed information, see Magnusson (2000).

Anchorage with different support conditions

Support conditions influence the anchorage behaviour significantly. The effect of support pressure acting perpendicular to the assumed split plane was studied in tests and finite element analyses of beam-ends; the specimens were either directly supported or indirectly supported as shown schematically in Fig. 8. Two or three ø16 bars were anchored in a 100 mm long anchorage region with a concrete cover of 16 mm. The normal-strength concrete specimens had two ø6 stirrups while the high-strength concrete specimens had two ø8 stirrups in the support region. The finite element mesh and boundary conditions adopted for the analyses are shown in Fig. 8.

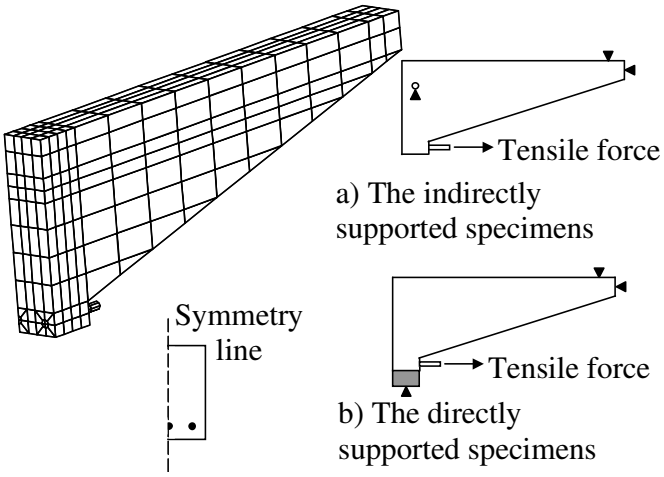

Figure 8 Finite Element Mesh and Boundary Conditions Adopted for the Analyses of the Beam-End Tests under Varying Support Conditions.

The tensile force versus end-slip relations, from the finite element analyses and from the tests of the specimens with two bars, are compared in Fig. 9. The notation gives information about the concrete type N or H; embedment length (100 mm); number of reinforcement bars, 2 or 3; direct or indirect support conditions, DS or IS; and that the test specimens contained stirrups S. Since the beam-ends were modelled using symmetry, the force in the two corner bars is the same in the analyses. Consequently, the tensile forces in the two corner bars are represented by one curve designated FEA 1,3.

It was concluded that the two support situations, with and without transverse pressure, give rise to two different stress states in the anchorage region. The transverse support pressure, caused by the support reaction in the directly supported beam-ends, provides for a more favourable stress state than that in the indirectly supported specimens. The value of the maximum tensile force obtained from the analyses was always closer to the higher of the two values registered in the tests; even so, the agreement between analyses and tests was good in general. A comparison of the analyses and the tests of the indirectly supported specimens (N100-2IS-S and H100-2IS-S) shows good agreement up to maximum load; also the post-peak behaviour was described in a satisfactory manner.

In the analysis of the directly supported normal-strength concrete specimen, N100-2DS-S, the increased stiffness of the ascending branch, caused by the transverse pressure, was simulated well; however, the model somewhat overestimated the maximum tensile force. The agreement between the test and analysis of the corresponding high-strength concrete specimen, H100-2DS-S, was good. For this specimen, in both the test and the analysis, the yield capacity of the reinforcement, F_{sy} = 115 kN, was reached prior to failure.

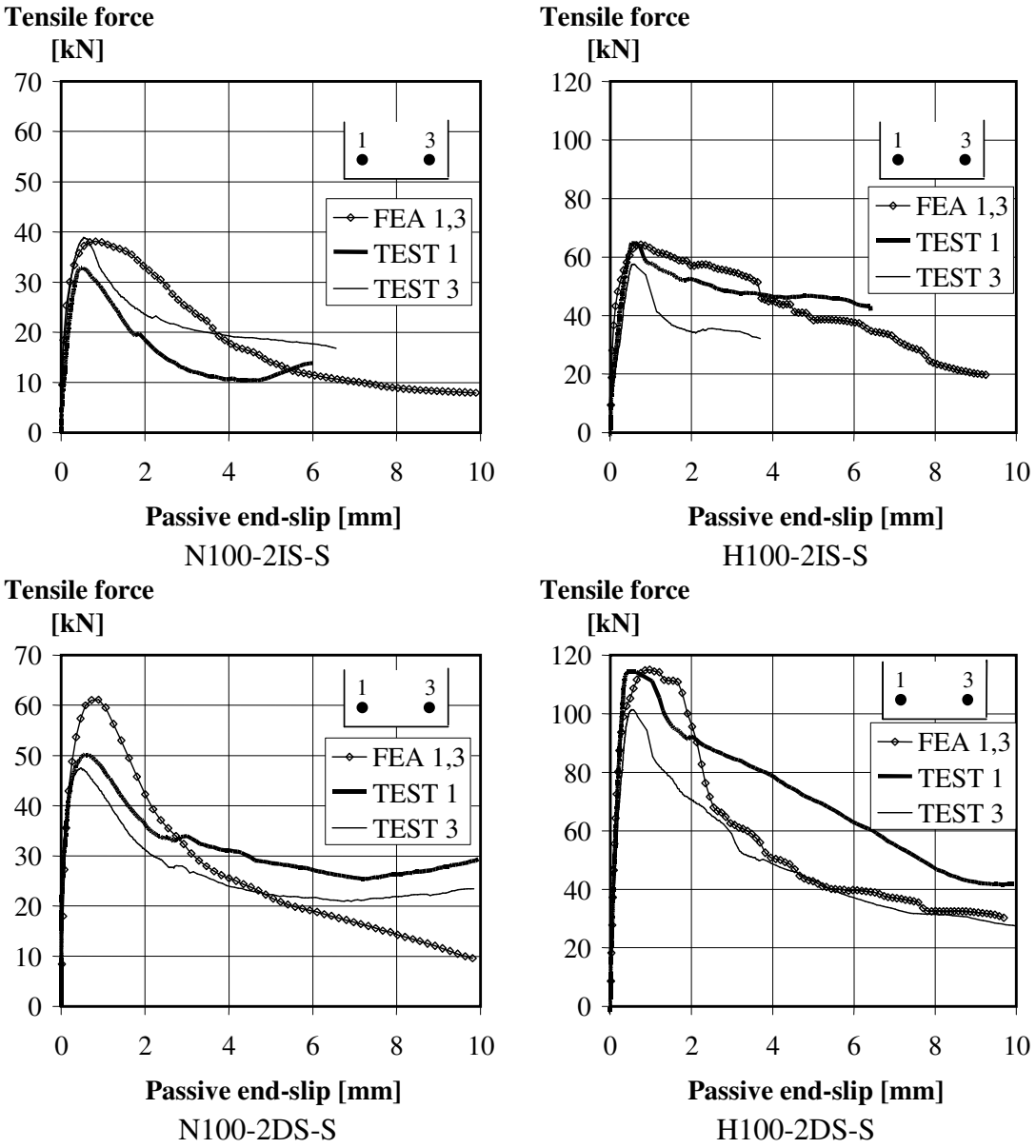

Figure 9 Test Results (TEST) from Beam-End Tests with Two Bars in Comparison with Numerical Predictions (FEA).

Anchorage at end region of simply supported beams

Several tests of simply supported beams subjected to four-point bending were carried out. Here, two tests that have been analysed will be discussed, one with normal-strength concrete, NSC-21, and one with high-strength concrete, HSC-21. Both beams were under-reinforced and contained four K500ST ø20 bars as tensile

reinforcement. The concrete cover was 20 mm and stirrups of the reinforcement type K500 ST ø6 were provided, one over the support and three in the shear span. Fig. 10 shows the mesh and the boundary conditions adopted.

The possibilities for stress redistribution were studied in finite element analyses. In Fig. 11 a comparison is made between the tensile force versus end-slip relations obtained from the tests and the analyses of beams NSC-21 and HSC-21. The comparison was done for cross-sections 130 mm from the end of the beams; i.e. outside the support region. The reason for this choice was that in this section all strain gauges attached to the main bars produced consistent results up to maximum load, which was not the case closer to the supports. The tensile forces from the tests were calculated using the results from the strain gauges. In general the test results ceased at maximum load, since the strain gauges were lost when the anchorage failed. The relations from the analyses were determined at the nodes in the centre of the bars. The agreement between analyses and tests is good, especially for the normal-strength concrete beam. The tensile force in the centre bars was higher than the force in the corner bars, in both analyses and tests.

The shape of the relations obtained from the analyses suggests that the anchorage failure of HSC-21 was more brittle than that of NSC-21. In the analyses of NSC-21 the confinement seemed sufficient for a rather ductile pull-out behaviour, although both radial splitting cracks and a global horizontal splitting crack between the bars had developed. For HSC-21 the same crack development was detected, but the anchorage behaviour was more brittle and, since the bond is modelled as a function of the available confinement, this appears to be the limiting factor. This can probably be related to the different tensile properties of the two concrete types, i.e. the relation between tensile strength and fracture energy.

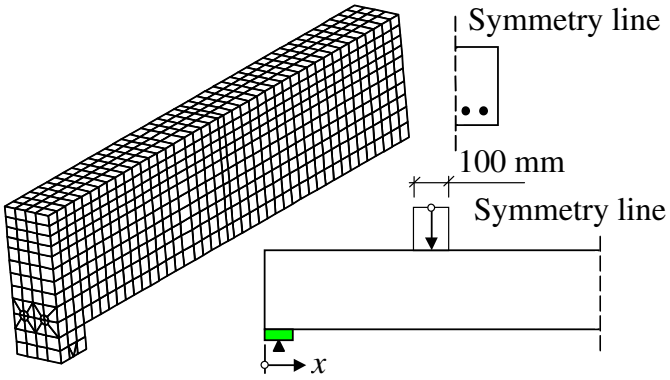

Figure 10 Finite Element Mesh and Boundary Conditions Adopted for the Analyses of the Beam Tests.

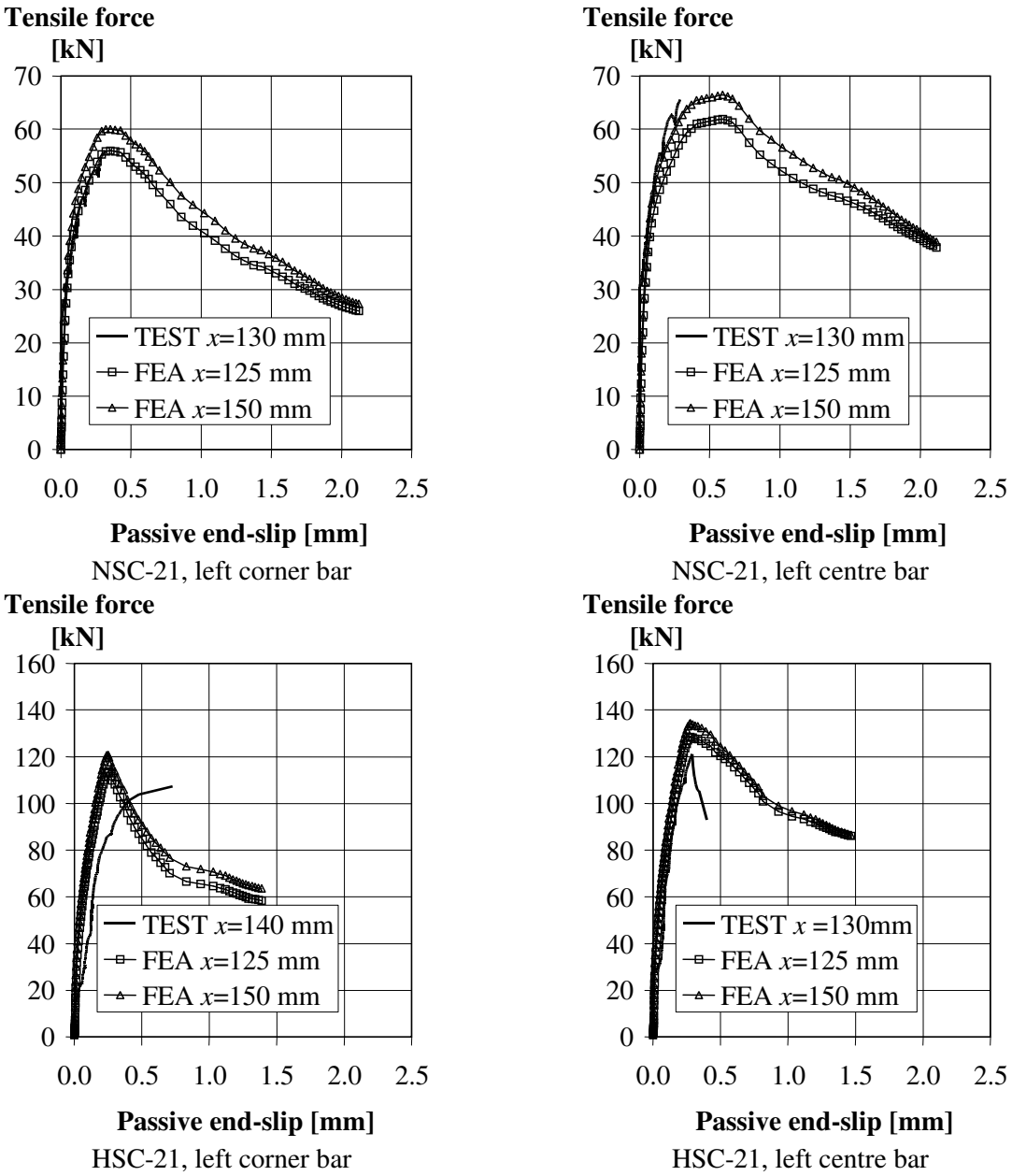

Figure 11 Tensile Force, at a Distance x From the End of the Beam, Versus Passive End-Slip from the Tests and Analyses of NSC-21 and HSC-21.

In the analyses of NSC-21, the maximum tensile force in the corner bars was reached well before the maximum load was reached, while the maximum tensile force in the centre bars was reached well after maximum load. For HSC-21, the maximum tensile force in the corner bars and the maximum load were reached at the same time, while the maximum tensile force in the centre bars was reached just after that. This suggests that there was redistribution of forces between the bars in both analyses, although the ability to redistribute forces was less in HSC-21 than in NSC-21.

The bond stress distributions obtained in the analyses are compared in Fig. 12. The main part of the force transfer between reinforcement and concrete took place above or close to the support, as was also observed in tests, see Magnusson (2000). The bond stress distributions for the high- and normal-strength concrete beams, at the same load levels, were similar. However, when comparing the bond stress distributions at maximum load, it is obvious that there was a much more uneven bond stress distribution at failure for HSC-21 than for NSC-21. This is also in agreement with the findings from the experimental studies.

CONCLUSIONS

The developed bond model was used in detailed three-dimensional analyses of anchorage regions. The analyses of beams with all reinforcement spliced with lap splices in the mid-span, together with analyses of a frame corner, with a reinforcement splice short enough to be limiting, show when compared with test results that the fracture of a lapped splice could be described in a reasonable way. The increase in strength and ductility due to stirrups along a splice was described by the analyses. The analyses of beam ends show that the effect of outer pressure is well described by the model. When no additional confinement from the support reaction was present, the development of splitting cracks reduced the anchorage capacity both in the analyses and in the tests. Also when additional confinement was provided by the support reaction, splitting cracks developed; however, they could be balanced by the transverse pressure and thus a higher capacity was obtained both in analyses and tests. The analyses show that the main part of the tensile force transfer between reinforcement and concrete takes place above or close to the support, as was also indicated in test results.

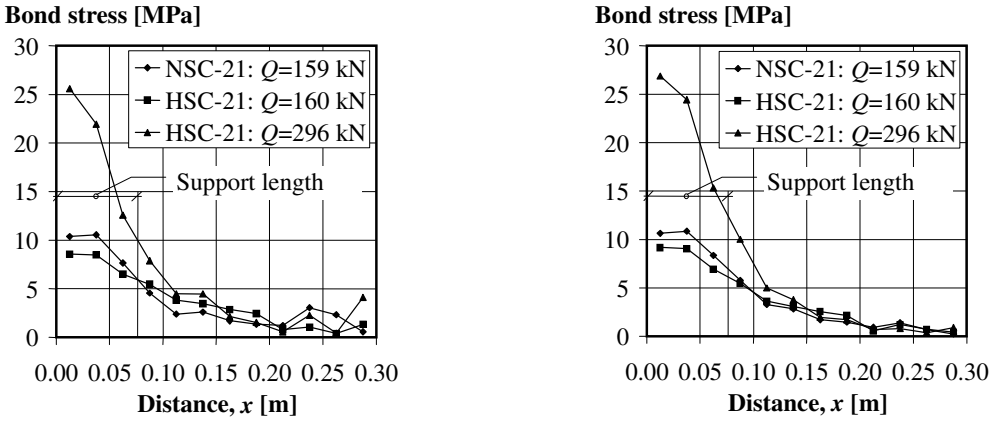

Figure 12 Bond Stress Distributions Obtained from the Analysis of NSC-21 (Anchorage Failure at Q = 159 kN) and HSC-21 (Anchorage Failure at Q = 296 kN).

The model was earlier calibrated for normal-strength concrete, but the analyses here show that this calibration also gives satisfactory results for high-strength concrete. The anchorage capacity of a high-strength concrete specimen was higher than that of a comparable normal-strength specimen, however, the behaviour of the high-strength concrete specimens was, in general, more brittle. Moreover, the analyses of anchorage at the end region of simply supported beams suggested that in the high-strength concrete beam it was difficult to redistribute the tensile forces between the anchored bars. This can most likely be related to the different tensile properties, i.e. the relation between tensile strength and fracture energy, of the two concrete types analysed. Furthermore, it was observed that the bond stress distribution at failure was more uneven for high-strength concrete than for normal strength concrete.

Since all of the analyses corresponded well with the measured responses, it can be concluded that the developed bond model could describe the behaviour of the different anchorage situations in a satisfactory way, and thus can be used for further studies of different anchorage situations.

REFERENCES

CEB (1995): *High Performance Concrete, Recommended Extensions to the Model Code 90, Research Needs.* Bulletin d'Information 228, Lausanne, Switzerland.

CEB (1993): *CEB-FIP Model Code 1990*. Bulletin d'Information 213/214, Lausanne, Switzerland.

Cox, J. V. and Herrmann L. R. (1999*)*: Validation of a plasticity bond model for steel reinforcement. *Mechanics of Cohesive-Frictional Materials*. Vol. 4, July 1999.

Cox, J. V. and Herrmann L. R. (1998*)*: Development of a plasticity bond model for steel reinforcement. *Mechanics of Cohesive-Frictional Materials*. Vol. 3, April 1998.

Cox, J. V. (1994*)*: *Development of a Plasticity Bond Model for Reinforced Concrete – Theory and Validation for Monotonic Applications*. Naval Facilities Engineering Service Centre, Port Hueneme, USA.

Lundgren, K. and Gylltoft, K. (2000): A model for the bond between concrete and reinforcement. *Magazine of Concrete Research*, Vol. 52, No. 1, Feb. 2000.

Lundgren, K. (1999): *Three-Dimensional Modelling of Bond in Reinforced Concrete: Theoretical Model, Experiments and Applications*. Ph. D. Thesis. Publication 99:1, Division of Concrete Structures, Chalmers University of Technology, Göteborg, Sweden.

Magnusson, J. (2000): *Bond and Anchorage of Ribbed Bars in High-Strength Concrete*. Ph. D. Thesis. Publication 00:1, Division of Concrete Structures, Chalmers University of Technology, Göteborg, Sweden.

Robins, P. J. and Standish, I. G. (1984): The influence of lateral pressure upon anchorage bond. *Magazine of Concrete Research*, Vol. 36, No. 129, Dec. 1984.

Thorenfeldt, E., Tomaszewicz, A., Jensen, J. J. (1987): Mechanical Properties of High-Strength Concrete and Application in Design. In *Proceedings Utilization of High Strength Concrete*, Symposium in Stavanger, Norway. Tapir N-7034 Trondheim.

TNO Building and Construction Research (1998). *DIANA Finite Element Analysis, User's Manual release 7*, Hague.

Åkesson, M. (1993): *Fracture Mechanics Analysis of the Transmission Zone in Prestressed Hollow Core Slabs*. Licentiate Thesis. Publication 93:5, Division of Concrete Structures, Chalmers University of Technology, Göteborg.